Circulation

IN DEPTH

Energetics of Blood Flow in Cardiovascular Disease

Concept and Clinical Implications of Adverse Energetics in Patients With a Fontan Circulation

ABSTRACT: Visualization and quantification of the adverse effects of distorted blood flow are important emerging fields in cardiology. Abnormal blood flow patterns can be seen in various cardiovascular diseases and are associated with increased energy loss. These adverse energetics can be measured and quantified using 3-dimensional blood flow data, derived from computational fluid dynamics and 4-dimensional flow magnetic resonance imaging, and provide new, promising hemodynamic markers. In patients with palliated single-ventricular heart defects, the Fontan circulation passively directs systemic venous return to the pulmonary circulation in the absence of a functional subpulmonary ventricle. Therefore, the Fontan circulation is highly dependent on favorable flow and energetics, and minimal energy loss is of great importance. A focus on reducing energy loss led to the introduction of the total cavopulmonary connection (TCPC) as an alternative to the classical Fontan connection. Subsequently, many studies have investigated energy loss in the TCPC, and energy-saving geometric factors have been implemented in clinical care. Great advances have been made in computational fluid dynamics modeling and can now be done in 3-dimensional patient-specific models with increasingly accurate boundary conditions. Furthermore, the implementation of 4-dimensional flow magnetic resonance imaging is promising and can be of complementary value to these models. Recently, correlations between energy loss in the TCPC and cardiac parameters and exercise intolerance have been reported. Furthermore, efficiency of blood flow through the TCPC is highly variable, and inefficient blood flow is of clinical importance by reducing cardiac output and increasing central venous pressure, thereby increasing the risk of experiencing the well-known Fontan complications. Energy loss in the TCPC will be an important new hemodynamic parameter in addition to other well-known risk factors such as pulmonary vascular resistance and can possibly be improved by patient-specific surgical design. This article describes the theoretical background of mechanical energy of blood flow in the cardiovascular system and the methods of calculating energy loss, and it gives an overview of geometric factors associated with energy efficiency in the TCPC and its implications on clinical outcome. Furthermore, the role of 4-dimensional flow magnetic resonance imaging and areas of future research are discussed.

Friso M. Rijnberg, MD
Mark G. Hazekamp, MD, PhD
Jolanda J. Wentzel, PhD
Patrick J.H. de Koning, Msc
Jos J.M. Westenberg, PhD
Monique R.M. Jongbloed, MD, PhD
Nico A. Blom, MD, PhD
Arno A.W. Roest, MD, PhD

http://circ.ahajournals.org

Cardiology is flow.[1] The primary goal of the cardiovascular system is to drive, regulate, and maintain adequate blood flow throughout the body.[1] Blood flows because potential pressure energy (systolic blood pressure), predominantly generated by the ventricles, is converted into kinetic energy (ie, velocity) along its course through the body.[2] The ventricles must provide the flowing blood with enough energy to overcome the unavoidable frictional loss of energy throughout the circulation.[2] Energy-consuming abnormal blood flow patterns (eg, flow separation, flow collision, or helical flow)[3] caused by abnormal geometry (eg, vessel/valve stenosis or vessel aneurysms) provide an increased working load to the ventricles to maintain adequate flow throughout the cardiovascular system, which may ultimately result in heart failure.[4] Furthermore, blood flow induces mechanical forces on the vessel wall. Abnormal values of these forces, for example, wall shear stress, have been identified in diseases such as atherosclerosis and aortic aneurysms.[1,5]

The degree of energy loss, and thereby its hemodynamic impact, is conventionally assessed with indirect, global parameters, such as vessel size, pressure gradients or effective orifice area, which may lead to inaccurate disease severity characterization.[2,4–6] Although visualization and direct measurement of 3-dimensional (3D) blood flow have long been elusive goals, emerging techniques such as four-dimensional flow magnetic resonance imaging (4D flow MRI) and patient-specific computational fluid dynamics (CFD) models are providing unprecedented, unique insights into physiological and pathophysiological flow in the human circulation. These techniques provide a time-resolved (ie, during a cardiac cycle) 3D velocity vector field (from 4D flow MRI) or a combined velocity and pressure field (from CFD).[5,7,8] Using these techniques, complex intracardiac and vascular flow patterns, including vortex formation and helical flow, have been identified in various cardiovascular diseases, including ischemic and dilated cardiomyopathies, aortic disease, valvular disease, and congenital heart disease.[6,7,9,10] Moreover, these techniques allow direct quantification of the energetics of the 3D, time-resolved blood flow data that lead to new hemodynamic parameters, such as viscous energy loss, turbulent kinetic energy, wall shear stress and kinetic energy.[8] Direct measurement of viscous energy loss (laminar flow) or turbulent kinetic energy (turbulent flow) in patients with aortic valve disease or aortic dilatation also takes the hemodynamic impact of the abnormal, energy-consuming flow patterns in the ascending aorta and aortic arch into account and may therefore better reflect disease severity complementary to conventional parameters.[6,11] The definitive role of these and other new energetic markers of blood flow in clinical decision making in various types of cardiovascular disease is promising and subject to future studies.

In patients with palliated single-ventricular heart defects, the Fontan circulation passively directs systemic venous return to the pulmonary circulation in the absence of a functional subpulmonary ventricle. The Fontan circulation is especially dependent on favorable flow and energetics, and minimal energy loss is of great importance. Minimizing energy loss, via the rationale that an energy-efficient total cavopulmonary connection (TCPC) leads to reduced central venous pressure and increased preload, and therefore cardiac output, aims to decrease the risk of well-known Fontan complications such as exercise intolerance, heart failure, protein-losing enteropathy, venovenous collateral formation, or liver fibrosis/cirrhosis.[12,13] The concept and clinical implications of adverse energetics in patients with a Fontan circulation are the subject of this article, including the theoretical background and methods of calculating energy loss, factors associated with increased/reduced energy loss and the correlation with clinical parameters.

THE FONTAN PROCEDURE

The Fontan procedure is the current standard palliative treatment of children with a functional univentricular heart. It creates a circulation system in which systemic venous return enters the pulmonary circulation passively, without the support of a cardiac ventricle. Originally, the procedure incorporated the right atrium into the design in a so-called atriopulmonary connection, with the rationale that contraction of the atrium can add forward energy to the otherwise passive flow entering the lungs. However, in a landmark in vitro study by de Leval et al,[14] it was shown that by incorporating a pulsatile atrium, turbulent flow inside this atrium led to increased rather than decreased energy loss, and the importance of energy efficiency was emphasized. It led to the recommendation of the TCPC, and subsequently its superiority over the atriopulmonary connection in terms of efficiency was demonstrated.[14–16] Today, the Fontan circulation is created in a staged approach. Most often a bidirectional cavopulmonary connection is performed by connecting the superior vena cava (SVC) end to side to the right pulmonary artery (RPA) at 6 to 12 months of age (Glenn), with completion of the Fontan circulation (TCPC) using an intraatrial lateral tunnel or extracardiac conduit (ECC) technique at 3 to 5 years of age. Some centers use the so-called hemi-Fontan procedure instead of the Glenn procedure, in which the SVC is not disconnected from the right atrium, but instead a patch reconstruction is performed between the medial side of the SVC, the right atrium, and the RPA. A second patch at the superior cavo-atrial junction prevents the blood flow from the inferior vena cava (IVC) from entering the PAs. With completion of the TCPC, this latter patch is removed and an intraatrial lateral tunnel is constructed,

allowing IVC flow toward the PAs. Therefore, final geometry and flow characteristics between patients with an intraatrial lateral tunnel Fontan after Glenn or Hemi-Fontan are inherently different.

The TCPC has 2 important tasks: it has to (1) be as energy efficient as possible, and (2) distribute hepatic blood to both lungs.[17] Adding IVC blood to the SVC flow from the bidirectional Glenn shunt makes for an almost complete separation of the pulmonary and systemic circulations. Only venous blood from the coronary circulation remains entering into the systemic circulation. Furthermore, IVC blood contains the important hepatic factor. A lack of this hepatic factor is associated with the formation of pulmonary arteriovenous malformations because a high prevalence has been reported after a Glenn shunt or a Kawashima procedure, with reduction of these pulmonary arteriovenous malformations after reincorporation of the hepatic veins into the Fontan circulation.[18]

Although short-term outcome after the Fontan procedure has improved considerably since its introduction in 1971,[12] long-term morbidity and mortality remain significant, including a generally limited exercise tolerance.[13,19]

Blood flow to the pulmonary vasculature in a patient with a Fontan is mainly driven by increased systemic venous pressure, which is formed by the remaining energy generated by the heart, the peripheral muscle pump, and intrathoracic pressure changes during respiration.[20] Because of the assumed importance of minimizing energy loss, the TCPC has been an area of extensive research. This has been done mainly via in vitro models,[9,14,21–34] CFD models,[3,9,16,17,26,27,30–67] and in vivo studies.[10,15,34,68–70] In the past 10 years, growing evidence suggests a relationship between energy loss in the TCPC and Fontan hemodynamics[47,59–62,69] and exercise tolerance.[63,66] To date, the influence of energy loss on other well-known complications such as protein-losing enteropathy, plastic bronchitis, or liver fibrosis/cirrhosis has not been studied.

Energy Loss Within the TCPC

The theoretical background of mechanical energy in human circulation and the methods of calculating and comparing energy loss are supplemented in Appendix I and II in the online-only Data Supplement.

Because the TCPC is basically a connection with 2 T junctions with opposite flow directions, sudden changes in velocities and directions of flow around corners and over decreasing cross-sectional areas (eg, PAs and branching) will inevitably lead to energy losses.[35,71] These energy losses are predominantly through viscous dissipation (Appendix I in the online-only Data Supplement) in laminar flow, although energy losses can be of greater magnitude when turbulent flow (Appendix III in the online-only Data Supplement) occurs.[2]

The intrinsic instability of TCPC flow has been observed in multiple studies.[3,22,26,30,31,68,72] With CFD, when using steady inflow boundary conditions, a highly disorganized and unsteady flow still appeared in the area of colliding blood flow from the SVC and IVC, extending into the PAs.[31] This includes areas of flow stagnation, formation of vortices, and the occurrence of swirling, helical flow patterns (Videos 1 and 2 in the online-only Data Supplement) into the PAs (Figure 1). Furthermore, these flow phenomena have been reported to change with varying cardiac outputs and RPA:LPA flow splits (the percentage of total caval blood flow to each PA branch). These flow patterns are characterized by high undo velocity gradients and are therefore highly dissipative, leading to increased energy loss in the TCPC.[3] Furthermore, wall shear stress has also been identified as a major contributor of energy loss,[43] with most energy being dissipated near the PA walls[26] and the corners of the anastomosis.[56]

Some studies have questioned the relevance of the energy loss in the TCPC because energy loss is generally low (Table) and may only contribute a small part to the whole energy loss in the pulmonary circulation.

In 1 study, energy loss in the TCPC during rest represented only 13% to 20% of energy loss in the pulmonary circulation and only 2% of ventricular power.[58,60] However, others have shown that TCPC resistance is highly variable and can be as high as 55% of pulmonary vascular resistance (PVR) in rest and increase up to 155% of PVR during simulated exercise.[47] In a recent study by Tang et al[66] reporting on TCPC energy loss in 47 patients during exercise, TCPC resistance index (RI) was on average 0.58 Woods Unit (WU) but could be as high as 2.23 WU.

Magnitude of Energy Loss

The range of calculated energy losses (in milliwatts) and, when available, the values of efficiency, resistance, RI, or indexed power loss (iPL) in 3D, patient-specific TCPC models are reported in the Table. Explanations of comparing TCPC efficiency using resistance, RI, and iPL are covered in Appendix II in the online-only Data Supplement. Efficiency of the TCPC (ie, the energy of outflowing versus inflowing blood [efficiency = energy out/energy in [%], in which the difference is caused by viscous energy loss in the TCPC) is highly variable between patients and ranges between 63% and 98% at rest and 63% to 91% during exercise (Table). TCPC RI is also highly variable and ranges between 0.05 and 1.6 WU (Appendix II in the online-only Data Supplement) at rest and between 0.07 and 3.95 WU during exercise. To put this in perspective, in patients with a Fontan circulation, PVR has been reported to be 1.9 to 2.8 WU (range 1.0–4.3).[47,77] IPL ranged from 0.007 to 0.122 in resting conditions, showing that iPL can be 12.2 to 16.7 times higher in the least efficient TCPCs compared with the most efficient TCPCs at rest.[60,62]
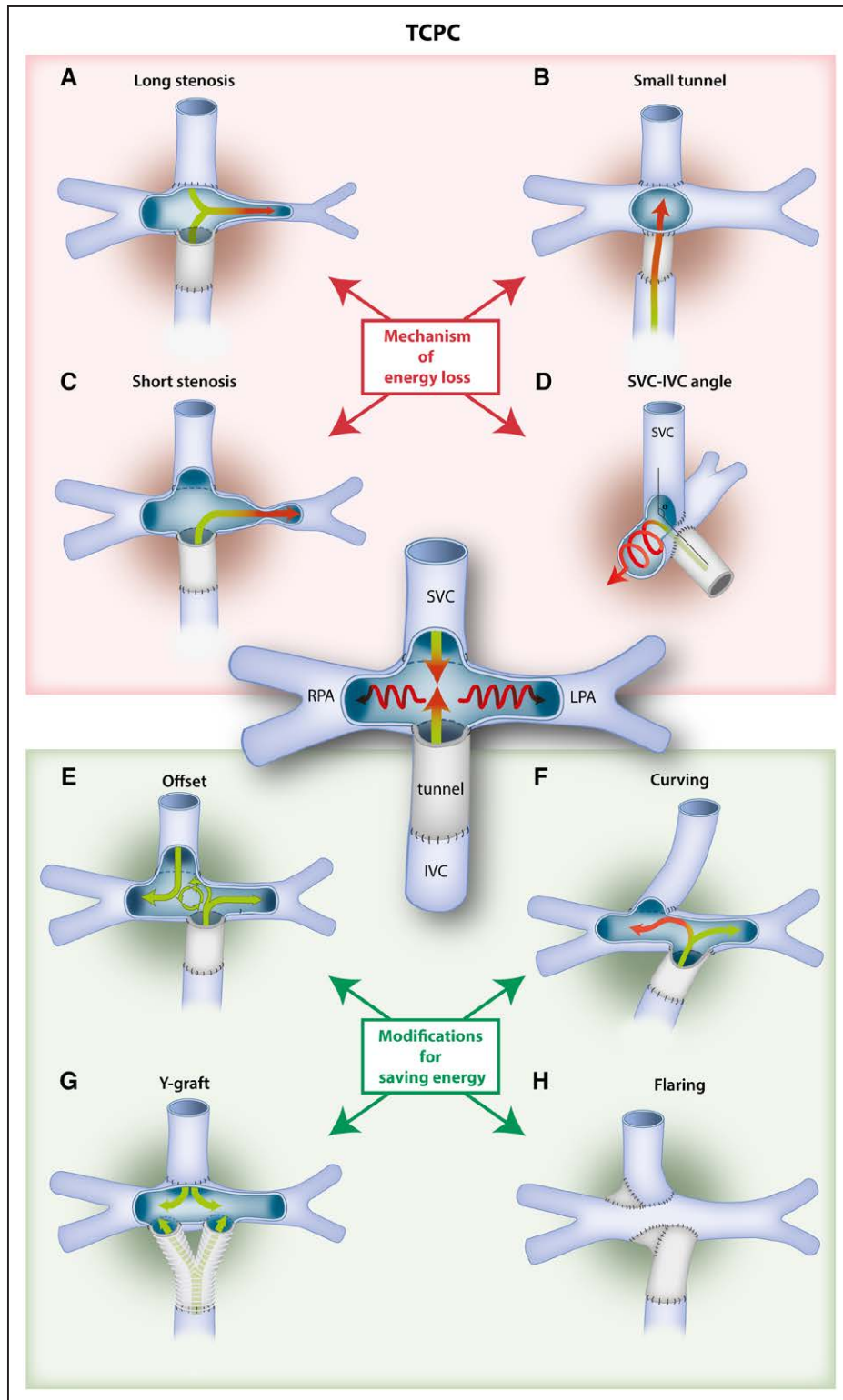
Figure 1. Geometric factors associated with increased energy loss in the TCPC and modifications to reduce energy loss in the TCPC.

Geometric factors associated with increased (**upper**) and decreased energy loss (**lower**) are depicted with a simplified, schematic extracardiac conduit TCPC (see text for further details). The same factors apply for lateral tunnel (LT) TCPCs. Colored arrows represent blood flow, and changes from green to red represent an increase in energy loss. When the inferior vena cava (IVC) and superior vena cava (SVC) are connected to the pulmonary vasculature directly opposite each other, collision of blood flow leads to a highly disorganized flow, with areas of flow stagnation and flow separation and the occurrence of a swirling, helical flow into the pulmonary arteries (PAs) (central figure). **Upper,** Geometric factors associated with increased energy (*Continued*)

Factors Influencing Energy Loss in the TCPC

Vessel Size

The effect of vessel size on energy loss has been reported in the TCPC,[26,30,61,64,66,78] and is a logical result of the law of Hagen–Poiseuille, which states that with a laminar, steady flow, the resistance of flow through a blood vessel is inversely proportional to the fourth power of the radius.

The effect of small, hypoplastic, or stenotic PAs (Figure 1A and 1C) are, together with the Fontan pathway diameter (Figure 1B),[61] the most important geometry factors associated with increased energy loss.[42,46,50,53,61,79] Pekkan et al[42] performed a virtual angioplasty of a short LPA stenosis of 85%, which led to a 50% decrease of energy dissipation when the stenosis was virtually widened. It was also shown that diffuse (long-segment) PA stenosis is more dissipative than a short stenosis.[42] This furthermore highlights the importance of well-developed PAs because in small PAs blood flow velocity will increase, leading to high wall shear stress and increased energy loss.[30,43,61]

Additionally, the effect of conduit sizes in patients with an ECC on energy loss has been studied. Hsia et al[40] modeled 5 conduit sizes from 10 to 30 mm and showed decreased energy loss with increasing conduit size to 20 mm. However, an increased conduit size of 30 mm resulted in increased energy loss because of increased flow recirculation within the conduit. Therefore, although small vessels are detrimental in terms of energy loss, bigger is not always better. These areas of flow stagnation or recirculation increase energy loss and may also increase the risk of thrombosis.[80]

Itatani et al[40,48] recommended 16- to 18-mm conduits for children 2 to 3 years of age, but whether this size was also ideal for adult patients was not investigated. The ideal conduit size will probably be patient-specific, and efficiency will change while the patient grows. The size of the used conduit will likely be limited by the conduit:IVC ratio because an increase in this ratio was associated with increased energy loss because of flow separation through expansion of flow from the sudden increase in diameter from IVC to Fontan tunnel.[24] Despite the fact that cardiac cath-eterization studies often show absent or minimal (≤2 mm Hg) pressure gradients in patients with Fontan tunnel stenosis,[81] energy loss from such an obstruction may nevertheless be significant and can exceed the total energy loss through the lungs. Restoring normal diameter with stenting has been shown to dramatically reduce this energy loss.[82] This example illustrates the importance of energy loss as a new, energetic marker because management based on pressure gradient can be misleading.

A recent study by Restrepo et al[64] showed that a TCPC inherently becomes more dissipative with age because it was reported that normalized vessel diameters (vessel diameters corrected for body surface area) decrease with time. In other words, growth of IVC, SVC, RPA, and LPA does not match somatic growth, making the TCPC less efficient with aging.

Total Blood Flow and Pulmonary Flow Split

Energy loss in the TCPC will be larger with an increase of blood flow, as demonstrated in multiple studies,[21,23,45,46,57,59,74] with energy loss increasing nonlinearly with an average of 10.5 and 38.9 times baseline energy loss with doubled and tripled flow mimicking exercise.[46] In that study, RI at rest (range 0.25–0.75 WU) increased nonlinearly (range 0.70-3.40 WU) during simulated exercise. In some patients, however, the simulated exercise conditions did not represent physiological values.

Pulmonary flow splits are anywhere near 55%:45% (RPA:LPA) in healthy humans and are derived from the mass ratio of the right and left lungs (ie, more blood flows normally through the bigger right lung).[17] Early in vitro studies with different simplified models have shown that the least energy loss is observed with 45% to 55% blood flow to the RPA, with increasing energy loss when flow splits are highly skewed toward 1 lung.[21,23] However, these values only apply for these specific models and conditions because models with other geometric properties show other optimal flow splits, ranging from 30% to 70% RPA flow.[26,30,32,46] For example, de Zelicourt et al[30] showed the least energy loss for a 70% RPA flow split because this patient-specific model had a small LPA. Increased flow through this LPA resulted in increased energy loss. Addition-

Figure 1 Continued. loss in the TCPC. The influence of a long or short PA stenosis (**A** and **C**) is illustrated, with a long, diffuse stenosis leading to more energy loss than a short, discrete stenosis. Together with a small Fontan tunnel (**B**), these are the most important factors associated with increased energy loss. The angle between the SVC and IVC influences the formation of swirling, helical flow patterns when angles are small (90 degrees), with improvement when angles are enlarged (150 degrees) (**D**). **Lower,** Modifications that reduce energy loss in the TCPC. Caval offset toward 1 of the PAs leads to less energy loss by avoiding flow collision and leads to the formation of a low-dissipative vortex (green circle), propelling blood flow into the PAs (**E**). Curving of the vena cava toward a PA leads to lower energy loss compared with an offset model without curving. However, when IVC flow split does not match pulmonary flow toward that PA, some flow has to make a sharp bend, increasing energy loss (red arrow) (**F**). Flaring of the anastomosis leads to reduced energy loss by avoiding dissipative sharp corners (**G**). The area-preserving Y graft allows for balanced hepatic blood flow split and is associated with reduced energy loss (**H**). TCPC indicates total cavopulmonary connection.

Table. Energy Loss in Realistic, Patient-Specific 3-Dimensional Models

Study	Year	Method	TCPC Models (n)	Flow (L/min)	Energy Loss (mW)	Efficiency % (Energy Out/ Energy In)	Resistance Index	Indexed Power Loss
Bove[39]	2003	CFD	2LT, 2ECC	2.29	4.1–56.6	—	—	—
Miggliavacci[73]	2003	CFD	4LT, 2ECC	2.28	15–55	—	—	—
Hsia[40]	2004	CFD	3LT, 6ECC	1.65	—	89–91	—	—
Pekkan[31]	2005	CFD, IVT	1IA	1–3	10–270	—	—	—
de Zelicourt[30]	2005	CFD	1IA	1–3	15–210	—	—	—
Pekkan[42]	2005	CFD	1ECC	2.6	15–230	—	—	—
Marsden[45]	2006	CFD	2ECC	2.16–6.24	6.7–13.9 (19.5–169.4)	75–93 (69–91)	—	—
de Zelicourt[9]	2006	CFD, IVT	2ECC	2–4	5–28 (34–70)	—	—	—
Whitehead[46]	2007	CFD	9IA, 1ECC	2.37–5.1 CI, ×2–3	5–20 (40–1200)*	—	0.25–0.75 (0.4–3.4)*	—
Sundareswaran[47]	2008	CFD	10ECC, 6IA	2–10.5	—	—	0.10–1.08 (0.13–2.65)	—
Marsden[49]	2009	CFD	2ECC, 2Y	1.9–5.6	—	87–90 (76–87)	—	—
Marsden[50]	2010	CFD	6ECC	1.6–3.8 CI, x2–3	—	74–96 (63–93)	—	—
Baretta[51]	2011	CFD	2ECC, 1Y	2.6 CI	1.09–4.80	91–96	—	—
Haggerty[54]	2012	CFD	1ECC, 3Y	2.6–3.3	1.3–5.1	—	0.18–0.35	—
Yang[74]	2012	CFD	8Y, 11ECC	1.3–2.5, x2–3	1.8–8.2 (2.9–32.5)	—	—	—
Ding[56]	2013	CFD	6ECC	NS	5.5–16*	—	—	—
Haggerty[57]	2013	CFD	5Y, 10ECC	3.0–3.8 CI, x2-3	—	—	0.15–1.60 (0.32–3.95)	—
Hong[75]	2014	CFD	1ECC, 1LT	NS	4.13–10.67	95–98	—	—
Sun[76]	2014	CFD	4ECC	2.48	4.5–13	81–95	—	—
Tang[61]	2013	CFD, IVT	1ECC	2.54	3.8–6.9	—	—	—
Honda[69]	2014	Catheterization	7ECC, 1IA, 1LT	NS	5.3–17.8	63–93	—	—
Haggerty[60]	2014	CFD	64IA, 33ECC	2.89–3.10 CI	—	—	0.05–0.66	0.007–0.117
Bossers[59]	2014	CFD	15LT, 14ECC	3.2–5.3 CI	Mean 1.4–3.2/m² (2.8–15.3/m²)	—	Mean 0.06–0.16 (0.07–0.28)	-
Khiabani[63]	2014	CFD	21IA, 9ECC	2.6–4.8 CI	—	—	—	Mean 0.04–0.05
Haggerty[62]	2015	CFD	25IA, 5ECC	3.2 CI	—	—	—	0.01–0.12
Restrepo[64]	2015	CFD	36LT, 12ECC	3.0–3.3CI	—	—	—	Mean 0.05–0.10
Cibis[70]	2015	4D MRI	2LT, 4ECC	NS	Mean 0.56	—	—	—
Trusty[65]	2016	CFD	30Y, 30ECC/LT	1.57–2.07	—	—	Mean 0.56–1.51†	—
Tang[66]	2017	CFD	33LT, 14ECC	Exercise, NS	—	—	Mean 0.58	Mean 0.05

Values are reported in ranges unless specified. Values in exercise conditions or simulated flow conditions >4 L/min are in parentheses. 4D MRI indicates four-dimensional magnetic resonance imaging; CFD, computational fluid dynamics; CI, cardiac index; ECC, extra cardiac conduit; IA, intraatrial lateral tunnel (after Hemi-Fontan); IVT, in vitro; LT, lateral tunnel (after Glenn); and NS, not specified.

*Estimation of values from published charts or graphics.

†Resistance (not indexed).

ally, Whitehead et al[46] reported increased energy loss for most patients when flow toward the LPA increased because in most patients the LPA is smaller than the RPA. However, in some patients, the effect of altering pulmonary flow split only had a minor effect on energy loss, and in others increasing LPA flow split resulted in decreased energy loss. In these latter patients, relative RPA hypoplasia was present. The pulmonary flow split in patients is therefore, when assuming equal PVR in each lung, predominantly caused by PA size, with most blood flowing through the biggest PA.[79] In other words, blood flow follows the path of least resistance, leading to skewed pulmonary flow splits when PA stenosis is present. Intuitively, in the ideal situation, total caval blood flow needs to be proportionally distributed over both pulmonary vascular beds. Restoring

PA diameter will restore a more balanced pulmonary flow split.[42]

Caval Flow Split

The previously mentioned studies stressed the importance of geometry (PA sizes) on optimal pulmonary flow split. In humans, IVC:SVC flow split changes from 51%:49% at birth, 45%:55% in children at 2.5 years of age, to the adult value of 65%:35% at 6.6 years of age.[83] Furthermore, lower limb exercise will predominantly increase IVC flow with ≤160%.[84,85] The effect of respiration on caval blood flow has also been reported, with IVC flow increasing with ≤60% to 87% during inspiration.[20,84] The influence of inspiration on SVC flow is less clearly established, varying from no increase in SVC flow to increase of flow with ≤90%.[20,84] Hjortdal et al[20] showed that in resting conditions, the caval flow split (IVC:SVC) was ≈70:30 during inspiration and 40:60 during expiration. During exercise, this ratio was 79:21 during inspiration and 64:36 during expiration.[85] Therefore, overall, but especially during lower limb exercise and inspiration, most blood will enter the TCPC via the IVC. An optimal connection of the IVC to the PAs will therefore be of great importance. For example, Ensley et al[22] modeled a connection in which the IVC was curved toward the RPA and the SVC toward the LPA. This resulted in low energy loss when pulmonary flow split to the RPA matched the caval flow split (ie, 60% IVC flow and 60% RPA flow). With lower RPA splits, energy loss increased because blood had to make a sharp bend from the curved IVC toward the LPA. A connection as such may be clinically unreliable because PVR can possibly change, influencing TCPC efficiency. For this same reason, connecting the IVC to a smaller LPA, while carrying the majority of flow, will likely not be the most efficient connection because blood flow has to be pushed through a smaller PA or make a sharp bend toward the RPA.

Proposed TCPC Modifications to Minimize Energy Loss

Offset IVC Versus SVC

The influence of an offset (Figure 1E) between the IVC and SVC connection has been studied to avoid the head collision of SVC and IVC flows, which has been shown to lead to highly disorganized secondary flow patterns, increasing energy dissipation.[21,22,25,29,68] Offsetting the venae cavae 1.0 to 1.5 diameters apart decreases energy loss ≤50% and has been repeatedly tested as the most efficient connection,[17,21,29,35,38] with even further reduction when the anastomosis site on the RPA is enlarged.[35,39] Such an offset leads to the formation of a beneficial, low-dissipative vortex between the IVC and SVC anastomosis, propelling their flow toward the respective PAs.[15,21,22,25,27]

Anastomosis Shape

Furthermore, the addition of curving (Figure 1F) or flaring (Figure 1H) of the anastomosis was investigated, showing that flaring of the IVC and SVC anastomosis, thereby avoiding dissipative sharp corners,[14,71] on all sides can reduce the energy loss with another 68% and was more efficient than a curvature of the SVC and IVC toward one PA.[22,23] The angle between the IVC and SVC connection and the shape of the anastomosis, a slot-like incision versus an oval excision, have been tested and had a significant influence on measured energy loss in those models, with ≤75% less energy loss when increasing the IVC-SVC angle from 90 to 150 degrees (Figure 1D), and ≤32% less energy loss over an oval-shaped excision versus a slot-like incision.[28,56] The avoidance of sharp corners and large differences in cross-sectional areas have been emphasized to maximize energy efficiency.[71]

Besides previously mentioned factors, multiple other modifications have been proposed for improving TCPC efficiency while keeping adequate hepatic flow distribution (HFD) to both lungs. Soerensen et al[86] proposed a so-called OptiFlo connection, in which both SVC and IVC were split toward both PAs, and this was shown to be 42% more efficient compared with the offset model. However, clinical implementation was considered to be difficult because of anatomic constraints and the need for large areas of non-native tissue. To address those drawbacks, the Y graft was introduced (Figure 1G).[49] Although the Y graft showed decreased energy loss compared with the T-junction TCPC in that study, a recent study of 30 implanted Y grafts showed that the TCPC resistance, including the Y graft, was ≈3 times higher than traditional ECC or lateral tunnel TCPCs at rest and during exercise conditions, making this commercially available Y graft inferior to the traditional TCPCs.[65,87] The main reason for this adverse result was the use of commercially available Y grafts, where the diameters of the 2 branches of the Y graft were half the diameter of the base. This effectively reduces the cross-sectional area with 50% and therefore acts as a long-segment obstruction. The use of area-preserving Y grafts should give better results and is a promising area for future research.[74]

A flow divider has also been tested in a CFD model, in which a flow-dividing device is placed inside the normal Fontan tunnel to mimic the effect of a Y graft and has been shown to reduce energy loss.[88]

HEPATIC FLOW DISTRIBUTION

Besides the importance of an energy-efficient TCPC, balanced HFD is needed to prevent the formation of pulmonary arteriovenous malformations in the hepatic factor-deprived lung. Dasi et al[52] identified caval offsetting as the main factor associated with unbalanced HFD in patients with an ECC because the SVC flow creates a momentum barrier for the IVC flow to cross toward the

other PA, and this has subsequently been identified as one of the most important factors influencing HFD.[60,61] Therefore, offsetting of the IVC is faced with a trade-off situation between reducing energy loss, on the one hand, and unbalanced HFD, on the other hand. Pulmonary flow split also has been found to be correlated with HFD.[52,60,61] Therefore, these data suggest that clinicians should consider a low threshold for intervention when factors associated with unbalanced pulmonary flow split, most important PA stenosis,[61,79] are present because of its association with increased energy loss and unbalanced HFD. Pulmonary flow split has also been identified as the most important factor influencing HFD in patients with intraatrial lateral tunnel (after Hemi-Fontan). This is explained by increased mixing of hepatic and SVC blood flows in these patients, contrary to patients with an ECC, before flow enters the pulmonary circulation, leading to a strong correlation between HFD and pulmonary flow split (eg, if more blood flows through the right lung, then less hepatic blood flows through the left lung). Furthermore, Ding et al[56] illustrated that increasing the angle between RPA and IVC from 45 to 75 degrees improved HFD toward the RPA. In other words, curving (Figure 1F) of the IVC toward the LPA reduced HFD toward the RPA in this model. Also, an increase of the angle between the Fontan tunnel and the SVC has been shown to correlate with unbalanced HFD in patient-specific TCPC models.[61] However, Ding et al[56] investigated this Fontan tunnel-SVC angle experimentally in a TCPC CFD model, and although a decreased angle (Figure 1D) led to increased energy loss because of helical flow formation, a change of angle did not affect HFD.[56] This illustrates that the influence of certain geometric factors on HFD is patient-specific, emphasizing the need for patient-specific virtual modeling.[54,80]

However, to date it is not known what the minimum amount of hepatic flow is to prevent the formation of pulmonary arteriovenous malformations. Quantification of HFD in large, longitudinal follow-up series using 4D flow MRI[10] or CFD simulations[52] should provide answers to this question. The answers will help in choosing the best surgical options created with virtual surgery with minimal energy loss while only providing the necessary, minimal amount of hepatic flow. Although the use of novel Y grafts also aimed to induce more balanced HFD,[74] first results show highly variable HFD related to multiple geometric and hemodynamic factors, including pulmonary flow split and SVC position, emphasizing the need for patient-specific surgical planning when using these grafts.[65]

Limitations of Energy Loss Assessment

CFD Studies
CFD has been used extensively in the past 3 decades to model the hemodynamics and efficiency of the TCPC,

first in highly simplified symmetrical cross-like models and later with advances in computer power and modeling possibilities in 3D patient-specific, image-based TCPC geometries (Table). The necessary steps for a CFD simulation and the drawbacks and challenges of these steps in CFD modeling have been written about in detail in previous studies.[89] Boundary conditions have to be set accurately, and assumptions such as rigid vessel walls,[44,90] steady versus pulsatile inflow conditions,[38,55,60,67] and the influence of respiration[45] have been studied and can change conclusions. For example, many studies have assumed a steady flow of venous blood from the vena cava to the PAs because of an absent right ventricle. However, flow in the IVC can increase with ≤87% during inspiration in patients with an TCPC,[20,84,85] and the contribution of this unsteady inflow or pulsatility on calculated energy loss differs between patients.[55] It has been demonstrated that IVC flow pulsatility changes significantly when changing from breath-held to free-breathing MRI flow acquisitions, emphasizing the influence of respiration on flow.[84] Therefore, by limiting the evaluation by using steady flow assumptions, the reported energy loss can be different among patients, and this difference can affect the reported conclusions. In other words, although significant advances have been made, the capability of a CFD model to compute realistic pressure and velocity fields in the TCPC depends on the accuracy and precision of the generated geometry and mesh, applied boundary conditions, and validity of the assumptions being made.

Besides that, large validation studies and larger series correlating CFD-derived parameters to clinical outcomes are needed. The capability of predictive modeling to improve outcome, which is one of the main advantages of CFD modeling in which clinicians can virtually test interventions or different surgical geometries in a patient-specific manner to determine the optimal treatment, needs to be confirmed in large series before clinical implementation can be considered.[91]

In Vitro Studies
Although in vitro modeling plays an important role in the research of TCPC energy loss, it should be realized that the early models, which demonstrated the importance of geometric factors such as caval offsetting and flaring on energy loss, included highly simplified, symmetrical, cross-like rigid tubes with uniform diameters.[14,21–24,26–28,78] Implementing more physiological features in these models, such as unequal vessel diameters and nonplanarity (ie, PAs do not lie in a strictly left to right plane) of the PAs, significantly changed fluid hemodynamics.[26] Besides the limiting, simplified geometry, most models also used steady inflow conditions and rigid materials influencing reported conclusions.[38,44,55,67,90] Patient-specific MRI-based TCPC models have led to more accurate models, although these

models still use rigid material and steady inflow conditions.[9,30,34] Recently, a promising in vitro model has been introduced that uses a patient-specific, MRI-derived compliant TCPC model based on the patient-specific compliance value and uses condition-specific (breath-held, free breathing and exercise), real-time, phase-contrast MRI-derived flow waveforms as inflow conditions.[92] First results have shown and quantified the effect of respiration and exercise on energy loss and demonstrated that the effect of these parameters was highly patient-specific. Therefore, it is emphasized that future CFD models should use patient- and condition-specific boundaries.

In Vivo Studies

Only a limited amount of in vivo studies has reported on calculated energy loss in the TCPC.[69,70,93] In vivo energy loss studies can be subdivided into studies using catheterization or 4D MRI-derived data to calculate energy loss. One advantage of these in vivo methods is that the number of assumptions to obtain the energy losses is limited compared with CFD modeling.

Catheterization Studies

The capability of the catheterization method to accurately capture the highly dynamic and 3D flow and pressure fields is limited. In a recent in vivo study,[69] averaged pressures and velocities were used at the inlet and outlet sections, which have been shown to overestimate energy loss with 18%,[94] and are inherently associated with measurement errors because the position and size of the catheter inside the vessel will influence measured pressure and velocity values. For example, when a swirling, helical flow pattern is present, the central pressure measurement may not reflect the true pressure. Also, when calculating the cross-sectional area of the vena cava and PAs, which is needed to calculate flow from velocity, vessels are assumed to be circular, which is not necessarily true. Furthermore, the possibility to calculate these losses during exercise is limited because catheterization with indwelling catheters[77] is not a routine practice.

4D Flow MRI Studies

One in vivo study used 4D flow MRI to calculate energy loss in the TCPC using the viscous dissipation method (Appendix I in the online-only Data Supplement), with an average energy loss of 0.56±0.28 milliwatts.[70] To date, 2 studies calculated kinetic energy using 4D flow MRI in the TCPC, with an average loss of 31±20% in 1 study[93] but an increase in kinetic energy of 142% in the other. In this latter study, the increase of kinetic energy is explained by a 50% decrease of the combined cross-sectional area of the SVC and IVC compared with the PAs.[95] It should be noted that kinetic energy is only part of the energy equation (Appendix I in the online-only Data Supplement) and does not represent total energy

loss. Although 4D flow MRI is a promising noninvasive technique that can be easily implemented in clinical care, spatial resolution (ie, the size of the voxels in mm³) is a major issue because this has been shown to be the limiting factor in accurately calculating energy loss (Appendix I in the online-only Data Supplement). However, although underestimating absolute true energy loss because of limited spatial resolution, the relative performance of the TCPC among subjects remains intact when compared with CFD values, indicating that comparison of subjects is still possible with 4D flow MRI.[70]

Clinical Relevance of Energy Loss in the TCPC

To date, increased energy loss in the TCPC has been linked to (1) reduced exercise capacity, and (2) altered cardiac parameters and increased central venous pressure (CVP).

Exercise Capacity and Energy Loss in the TCPC

Exercise capacity is generally limited in patients after a TCPC, with a peak oxygen consumption (Vo_2 max) of only 65% of expected at 12 years of age, which gradually worsens with increasing age.[13,96] However, there is considerable variability in exercise tolerance, varying from 19% of predicted Vo_2 max to even supranormal values, with only 28% of patients having a normal value.[13]

Although the lower exercise tolerance in patients with a Fontan circulation is multifactorial, including chronotropic incompetence, arterial desaturation, diastolic dysfunction, peripheral factors (eg, lean muscle mass), and SV stroke volume, the latter (stroke volume) has been marked as the most important factor, explaining ≤73% of variance in Vo_2 max among patients.[13,19,77]

The resting cardiac output (CO) in a patient with a Fontan circulation is generally 60% to 70% of predicted, and the ability to increase CO during exercise is severely impaired because of preload deprivation. The role of PVR as the main factor controlling CO by limiting preload has been well recognized.[97] The TCPC resistance can be seen as a separate resistance in series with the PVR. Because of the clear role of PVR on the disability to increase CO, the energy loss or resistance in the TCPC has been studied as a possible contributing factor of reduced CO and therefore reducing exercise tolerance via the same mechanism as PVR does.

In healthy adults, PVR has been shown to decrease ≤50% at exercise.[98] This means that the TCPC resistance (Appendix II in the online-only Data Supplement), although possibly of minor influence in resting conditions, can be the predominant bottleneck during exercise. In other words, the focus of PVR as the most important factor of influence on preload can shift during exercise conditions toward the TCPC resistance in some

patients because the TCPC resistance has been shown to increase exponentially with exercise.[46]

The only study to date showing a correlation between energy loss and exercise capacity in patients with TCPC is by Khiabani et al.[63] In this study, 30 patients performed metabolic exercise testing, and flow rates were collected during rest and exercise using MRI. A significant negative linear correlation ($r=-0.6$) was seen among iPL, Vo_2 max, and work (per kg). These results were later confirmed in an extension of this study in 47 patients.[66] In that study, the TCPC diameter index—an index capturing the minimal diameters of all the 4 TCPC vessels (IVC, SVC, RPA, and LPA) in 1 parameter—showed a significant moderate correlation ($r=0.468$) with Vo_2 max.

In a study by Bossers et al,[59] MRI data were obtained from 29 patients during rest and during dobutamine infusion mimicking exercise. CFD models were constructed, and to simulate lower body exercise, 2x IVC flow was simulated. In this study, using RI and energy loss normalized by body surface area, no correlation was found between energy loss and exercise performance parameters. It has been suggested that normalizing energy loss with body surface area is the reason this study found no difference in exercise capacity because this parameter is highly flow-dependent.[99]

Cardiac Parameters and Energy Loss in the TCPC

In the last decade, a number of studies have reported correlations between energy loss within the TCPC and cardiac parameters and CVP.

In a lumped parameter model, Sundareswaran et al[47] showed a weak ($r=-0.36$) negative linear correlation between TCPC resistance and CO, with an expected CO decrease of 8.8% for each 10% increase in TCPC resistance. This finding was later confirmed in the largest series to date using CFD modeling, in which iPL was inversely correlated with cardiac index ($r=-0.21$) and systemic venous return ($r=-0.31$).[60] Additionally, a significant, moderate inverse relationship between iPL and end diastolic ($r=-0.48$), end systolic ($r=-0.37$), and stroke volumes ($r=-0.37$) was reported. Furthermore, a positive correlation was found between iPL and time to peak filling rate ($r=0.67$).[62]

Sundareswaran et al[47] reported both an increase in ventricular-vascular coupling mismatch and an increase of CVP with increasing TCPC resistance. CVP increased with 6.4% for each 10% increase in resistance. In a mathematical study using failing Fontan hemodynamics, 57% of the increase in CVP in patients with failing Fontan, defined as New York Heart Association classes III and IV, supraventricular tachyarrhythmias, persistent effusions unresponsive to diuretic therapy, and hypoalbuminemia, could be ascribed to TCPC resistance and the remaining increase to a rise of atrial pressure.[100]

In the only in vivo study to date correlating TCPC energetics with cardiac parameters, a positive correlation was found between energy loss measured during catheterization and time constant Tau and systolic dPdt (contractility), reflecting diastolic and systolic function, respectively. However, no correlation between energy loss and systemic venous flow was found.[69]

These data suggest the importance of energy loss in the TCPC on hemodynamics by reducing ventricular preload, preload reserve, and thereby CO, and possibly by influencing diastolic function.

FUTURE DIRECTIONS AND CONCLUSIONS

In the past 3 decades, the factors associated with the energetics in the TCPC and the potential role of this energy loss on Fontan outcome has become more obvious. However, although an increasing amount of studies connect energy loss with cardiac parameters and exercise capacity, evidence is mainly based on small (n ≤ 30) series, and some have conflicting results. Furthermore, to date, no studies connect complications associated with failing Fontan physiology, such as protein-losing enteropathy, plastic bronchitis, or liver cirrhosis with energy loss in the TCPC. Larger, multicenter series are needed, and long-term follow-up should definitely clarify the role of energy loss in the TCPC on long-term outcomes and can thereby possibly predict adverse outcomes early. Additionally, to date, energy loss is almost exclusively calculated via CFD modeling, and the capability of this method to reflect reality depends on the accuracy of the boundary conditions and the validity of underlying assumptions.

4D flow MRI can be of important complementary value by offering in vivo, noninvasive acquisition of accurate time-resolved 3D velocity vector fields (Videos 1 and 2 in the online-only Data Supplement), after which energy loss, kinetic energy, turbulent kinetic energy, and areas of increased wall shear stress in the TCPC can be calculated (Figure 2). However, main limitations include a long scan time, noisy velocity data, and limited spatial and temporal resolution. Increasing resolution to better capture 3D flow and velocity gradients will decrease signal to noise ratio and increase scanning time, and consequently its clinical use is now limited. New sequences for accelerating acquisition of data are developed and can reduce scan time, however, at a possible cost of reduced accuracy. For implementation of 4D flow MRI techniques in the patient with a Fontan circulation, optimal scan parameters and protocols have to be determined, in which compromises between resolution and clinical acceptable scanning times have to be made.[8]

Large 4D flow MRI series will be needed and should ideally put calculated TCPC resistance in the context
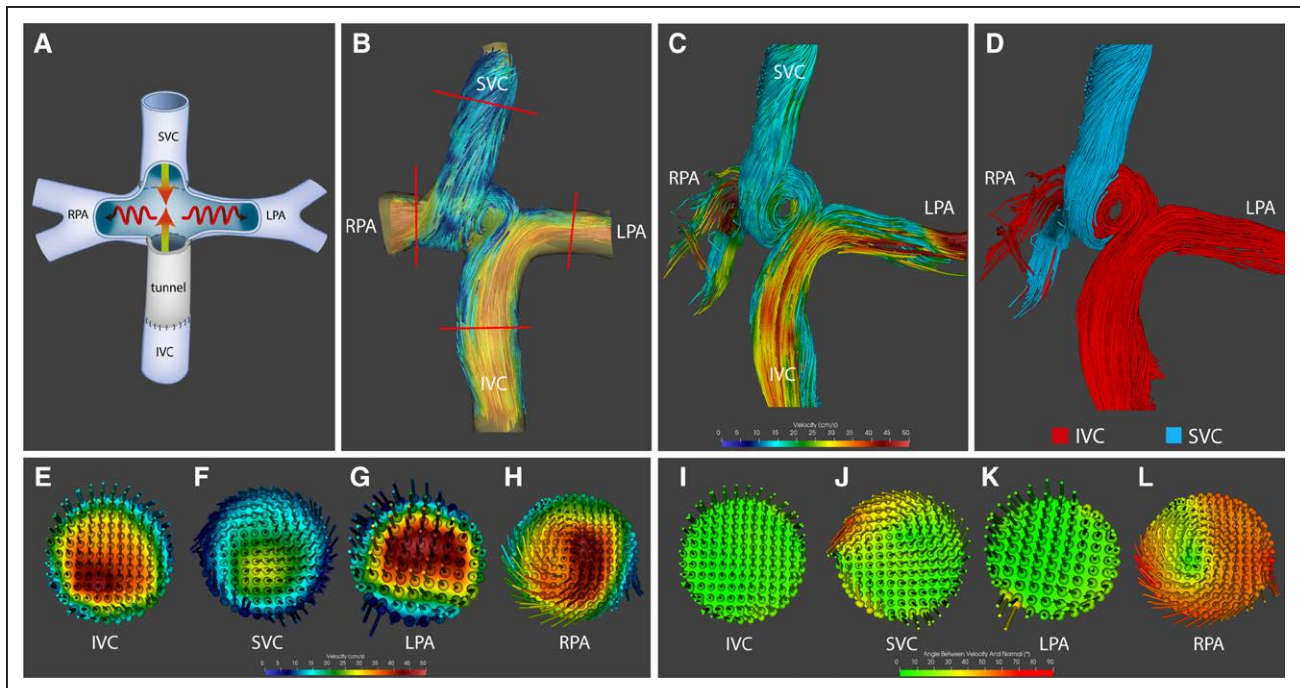
Figure 2. Visualization of abnormal blood flow patterns in the TCPC with 4D MRI.
Unprecedented possibilities of visualizing blood flow patterns in vivo in patients with a Fontan circulation by using 4D flow MRI. The schematic TCPC with zero offset (Figure 1) is shown for orientation (**A**). Images show the TCPC of an 18-year-old patient with tricuspid atresia with a nonfenestrated 16-mm extracardiac conduit with offset, leading to predominant inferior vena cava (IVC) flow toward the left pulmonary artery (LPA) (**B** through **L**). The orientation of the swirling blood flow within the crux of the TCPC and the location of the cross-sectional planes are shown (**B**). Streamlines and particle tracings are shown from a left anterior oblique view (**C** and **D**). Pathlines with velocity coding show areas of slow (blue) blood flow in the SVC and increased (red) velocities inside the tunnel and the distal PAs, with the formation of a swirling flow into the right pulmonary artery (RPA). Also, a swirling inflow from the vena anonyma (not included) into the proximal part of the SVC is noted (**C**). Particle tracing analysis shows the differential contribution and interaction between IVC and superior vena cava (SVC) blood flow. SVC flow is pushed anteriorly into the helical flow extending into the RPA. Additionally, SVC blood flows exclusively toward the RPA, and predominant SVC flow to the lower right segmental pulmonary artery is shown (**D**). The flow vectors are shown and visualized for velocity (**E** through **H**) and for the angle to the normal (the normal is the vector perpendicular to the plane) (**I** through **L**). Although most of the flow in the IVC, SVC, and LPA shows laminar flow with no angle (ie, blood flows parallel to the vessel wall), angles ≤70 degrees are shown in the RPA at the site of the helical flow. These abnormal flow patterns are associated with increased energy loss.[7] It is important to note that blood flow qualification (visualization) is only 1 of the many possibilities of 4D MRI. The acquired 4D flow data (velocity field) can also be used to calculate quantitative haemodynamic parameters based on these in vivo velocity data (in contrast with CFD) among which are energy loss and wall shear stress (not shown here). The figures were morphed for better display without editing the flow within the TCPC. 4D indicates four dimensional; MRI, magnetic resonance imaging; and TCPC, total cavopulmonary connection.

of patient-specific PVR, both at rest and during exercise conditions. Furthermore, large 4D flow MRI series should be obtained and used to validate CFD models in capturing the sometimes highly 3D chaotic flows, which to date have only been performed in a limited number of patients with a Fontan circulation.[34,60] Furthermore, confirmation of the impact of energy loss on clinical outcome based on in vivo data with 4D flow MRI will likely increase confidence in computed results from CFD studies and may accelerate the clinical implementation of patient-specific CFD models in the future.

In conclusion, an extensive amount of studies has shown that the efficiency of the TCPC is highly variable and therefore provides room for improvement. The

TCPC resistance will likely be an important additional parameter, complementary to factors such as PVR, in determining outcomes in patients with a Fontan circulation. Therefore, via the same rationale for why efforts have been made to decrease PVR in patients with a Fontan circulation, surgical modifications and patient-specific TCPC planning will aim to improve outcomes by reducing TCPC resistance and thereby increasing TCPC efficiency.

When a more definitive correlation between energy loss in the TCPC and adverse outcomes such as protein-losing enteropathy, plastic bronchitis, liver cirrhosis, and exercise intolerance has been clarified, knowledge about the factors explaining the variability of the TCPC

efficiency and the possibility of virtual surgery using CFD predictive modeling will likely guide future management in a patient-specific manner.

This review illustrates the important concept of adverse energetics in the TCPC in patients with a Fontan circulation. However, the same principles of visualization and quantification of 3D blood flow data and the adverse effects of distorted blood flow on energetics are promising in many cardiovascular diseases, including ischemic and dilated cardiomyopathies, valvular heart disease, aortic disease, heart failure, and other congenital heart disease. Future studies should clarify the role of these new parameters in various cardiovascular diseases to determine its potential use in clinical care.

ARTICLE INFORMATION

Correspondence

Arno A. W. Roest, MD, PhD, Department of Pediatric Cardiology, Leiden University Medical Center, Albinusdreef 2, 2333ZA, Leiden, The Netherlands. E-mail a.roest@lumc.nl

Affiliations

Department of Cardiothoracic Surgery (F.M.R., M.G.H.), Department of Radiology (P.J.H.d.K., J.J.M.W.), Department of Pediatric Cardiology (N.A.B., A.A.W.R.), and Departments of Cardiology and Anatomy and Embryology (M.R.M.J.), Leiden University Medical Center, The Netherlands. Department of Biomechanical Engineering, Erasmus Medical Center, Rotterdam, The Netherlands (J.J.W.).

Acknowledgments

Sources of Funding

Disclosures

None.

REFERENCES

1. Richter Y, Edelman ER. Cardiology is flow. *Circulation*. 2006;113:2679–2682. doi: 10.1161/CIRCULATIONAHA.106.632687.
2. Akins CW, Travis B, Yoganathan AP. Energy loss for evaluating heart valve performance. *J Thorac Cardiovasc Surg*. 2008;136:820–833. doi: 10.1016/j.jtcvs.2007.12.059.
3. Wang C, Pekkan K, de Zélicourt D, Horner M, Parihar A, Kulkarni A, Yoganathan AP. Progress in the CFD modeling of flow instabilities in anatomical total cavopulmonary connections. *Ann Biomed Eng*. 2007;35:1840–1856. doi: 10.1007/s10439-007-9356-0.
4. Dasi LP, Pekkan K, de Zelicourt D, Sundareswaran KS, Krishnankutty R, Delnido PJ, Yoganathan AP. Hemodynamic energy dissipation in the cardiovascular system: generalized theoretical analysis on disease states. *Ann Biomed Eng*. 2009;37:661–673. doi: 10.1007/s10439-009-9650-0.
5. Youssefi P, Sharma R, Figueroa CA, Jahangiri M. Functional assessment of thoracic aortic aneurysms: the future of risk prediction? *Br Med Bull*. 2017;121:61–71. doi: 10.1093/bmb/ldw049.
6. Barker AJ, van Ooij P, Bandi K, Garcia J, Albaghdadi M, McCarthy P, Bonow RO, Carr J, Collins J, Malaisrie SC, Markl M. Viscous energy loss in the presence of abnormal aortic flow. *Magn Reson Med*. 2014;72:620–628. doi: 10.1002/mrm.24962.
7. Calkoen EE, Roest AA, van der Geest RJ, de Roos A, Westenberg JJ. Cardiovascular function and flow by 4-dimensional magnetic resonance imaging techniques: new applications. *J Thorac Imaging*. 2014;29:185–196. doi: 10.1097/RTI.0000000000000068.
8. Dyverfeldt P, Bissell M, Barker AJ, Bolger AF, Carlhäll CJ, Ebbers T, Francios CJ, Frydrychowicz A, Geiger J, Giese D, Hope MD, Kilner PJ, Kozerke S, Myerson S, Neubauer S, Wieben O, Markl M. 4D flow cardiovascular magnetic resonance consensus statement. *J Cardiovasc Magn Reson*. 2015;17:72. doi: 10.1186/s12968-015-0174-5.
9. de Zélicourt DA, Pekkan K, Parks J, Kanter K, Fogel M, Yoganathan AP. Flow study of an extracardiac connection with persistent left superior vena cava. *J Thorac Cardiovasc Surg*. 2006;131:785–791. doi: 10.1016/j.jtcvs.2005.11.031.
10. Jarvis K, Schnell S, Barker AJ, Garcia J, Lorenz R, Rose M, Chowdhary V, Carr J, Robinson JD, Rigsby CK, Markl M. Evaluation of blood flow distribution asymmetry and vascular geometry in patients with Fontan circulation using 4-D flow MRI. *Pediatr Radiol*. 2016;46:1507–1519. doi: 10.1007/s00247-016-3654-3.
11. Binter C, Gotschy A, Sundermann SH, Frank M, Tanner FC, Luscher TF, Manka R, Kozerke S. Turbulent kinetic energy assessed by multipoint 4-dimensional flow magnetic resonance imaging provides additional information relative to echocardiography for the determination of aortic stenosis severity. *Circ Cardiovasc Imaging*. 2017;10:e005486. doi: 10.1161/CIRCIMAGING.116.005486.
12. d'Udekem Y, Iyengar AJ, Galati JC, Forsdick V, Weintraub RG, Wheaton GR, Bullock A, Justo RN, Grigg LE, Sholler GF, Hope S, Radford DJ, Gentles TL, Celermajer DS, Winlaw DS. Redefining expectations of long-term survival after the Fontan procedure: twenty-five years of follow-up from the entire population of Australia and New Zealand. *Circulation*. 2014;130(11 Suppl 1):S32–S38. doi: 10.1161/CIRCULATIONAHA.113.007764.
13. Paridon SM, Mitchell PD, Colan SD, Williams RV, Blaufox A, Li JS, Margossian R, Mital S, Russell J, Rhodes J; Pediatric Heart Network Investigators. A cross-sectional study of exercise performance during the first 2 decades of life after the Fontan operation. *J Am Coll Cardiol*. 2008;52:99–107. doi: 10.1016/j.jacc.2008.02.081.
14. de Leval MR, Kilner P, Gewillig M, Bull C. Total cavopulmonary connection: a logical alternative to atriopulmonary connection for complex Fontan operations: experimental studies and early clinical experience. *J Thorac Cardiovasc Surg*. 1988;96:682–695.
15. Be'eri E, Maier SE, Landzberg MJ, Chung T, Geva T. In vivo evaluation of Fontan pathway flow dynamics by multidimensional phase-velocity magnetic resonance imaging. *Circulation*. 1998;98:2873–2882.
16. Van Haesdonck JM, Mertens L, Sizaire R, Montas G, Purnode B, Daenen W, Crochet M, Gewillig M. Comparison by computerized numeric modeling of energy losses in different Fontan connections. *Circulation*. 1995;92(9 Suppl):II322–II326.
17. Dubini G, de Leval MR, Pietrabissa R, Montevecchi FM, Fumero R. A numerical fluid mechanical study of repaired congenital heart defects: application to the total cavopulmonary connection. *J Biomech*. 1996;29:111–121.
18. McElhinney DB, Kreutzer J, Lang P, Mayer JE Jr, del Nido PJ, Lock JE. Incorporation of the hepatic veins into the cavopulmonary circulation in patients with heterotaxy and pulmonary arteriovenous malformations after a Kawashima procedure. *Ann Thorac Surg*. 2005;80:1597–1603. doi: 10.1016/j.athoracsur.2005.05.101.
19. Goldberg DJ, Avitabile CM, McBride MG, Paridon SM. Exercise capacity in the Fontan circulation. *Cardiol Young*. 2013;23:824–830. doi: 10.1017/S1047951113001649.
20. Hjortdal VE, Emmertsen K, Stenbøg E, Fründ T, Schmidt MR, Kromann O, Sørensen K, Pedersen EM. Effects of exercise and respiration on blood flow in total cavopulmonary connection: a real-time magnetic resonance flow study. *Circulation*. 2003;108:1227–1231. doi: 10.1161/01.CIR.0000087406.27922.6B.
21. Sharma S, Goudy S, Walker P, Panchal S, Ensley A, Kanter K, Tam V, Fyfe D, Yoganathan A. In vitro flow experiments for determination of optimal geometry of total cavopulmonary connection for surgical repair of children with functional single ventricle. *J Am Coll Cardiol*. 1996;27:1264–1269. doi: 10.1016/0735-1097(95)00598-6.
22. Ensley AE, Lynch P, Chatzimavroudis GP, Lucas C, Sharma S, Yoganathan AP. Toward designing the optimal total cavopulmonary connection: an in vitro study. *Ann Thorac Surg*. 1999;68:1384–1390.

23. Gerdes A, Kunze J, Pfister G, Sievers HH. Addition of a small curvature reduces power losses across total cavopulmonary connections. *Ann Thorac Surg*. 1999;67:1760–1764.

24. Lardo AC, Webber SA, Friehs I, del Nido PJ, Cape EG. Fluid dynamic comparison of intra-atrial and extracardiac total cavopulmonary connections. *J Thorac Cardiovasc Surg*. 1999;117:697–704. doi: 10.1016/S0022-5223(99)70289-8.

25. Ensley AE, Ramuzat A, Healy TM, Chatzimavroudis GP, Lucas C, Sharma S, Pettigrew R, Yoganathan AP. Fluid mechanic assessment of the total cavopulmonary connection using magnetic resonance phase velocity mapping and digital particle image velocimetry. *Ann Biomed Eng*. 2000;28:1172–1183.

26. Ryu K, Healy TM, Ensley AE, Sharma S, Lucas C, Yoganathan AP. Importance of accurate geometry in the study of the total cavopulmonary connection: computational simulations and *in vitro* experiments. *Ann Biomed Eng*. 2001;29:844–853.

27. Amodeo A, Grigioni M, Oppido G, Daniele C, D'Avenio G, Pedrizzetti G, Giannico S, Filippelli S, Di Donato RM. The beneficial vortex and best spatial arrangement in total extracardiac cavopulmonary connection. *J Thorac Cardiovasc Surg*. 2002;124:471–478.

28. Gerdes A, Benthin U, Sievers HH. Influence of arteriotomy shape on power losses across *in vitro* cavopulmonary connections. *J Cardiovasc Surg (Torino)*. 2002;43:787–791.

29. Amodeo A, Grigioni M, D'Avenio G, Daniele C, Di Donato RM. The patterns of flow in the total extracardiac cavopulmonary connection. *Cardiol Young*. 2004;14(Suppl 3):53–56.

30. de Zélicourt DA, Pekkan K, Wills L, Kanter K, Forbess J, Sharma S, Fogel M, Yoganathan AP. *In vitro* flow analysis of a patient-specific intraatrial total cavopulmonary connection. *Ann Thorac Surg*. 2005;79:2094–2102. doi: 10.1016/j.athoracsur.2004.12.052.

31. Pekkan K, de Zélicourt D, Ge L, Sotiropoulos F, Frakes D, Fogel MA, Yoganathan AP. Physics-driven CFD modeling of complex anatomical cardiovascular flows-a TCPC case study. *Ann Biomed Eng*. 2005;33:284–300.

32. Soerensen DD, Pekkan K, de Zélicourt D, Sharma S, Kanter K, Fogel M, Yoganathan AP. Introduction of a new optimized total cavopulmonary connection. *Ann Thorac Surg*. 2007;83:2182–2190. doi: 10.1016/j.athoracsur.2006.12.079.

33. Tang E, Haggerty CM, Khiabani RH, de Zélicourt D, Kanter J, Sotiropoulos F, Fogel MA, Yoganathan AP. Numerical and experimental investigation of pulsatile hemodynamics in the total cavopulmonary connection. *J Biomech*. 2013;46:373–382. doi: 10.1016/j.jbiomech.2012.11.003.

34. Roldán-Alzate A, García-Rodríguez S, Anagnostopoulos PV, Srinivasan S, Wieben O, François CJ. Hemodynamic study of TCPC using *in vivo* and *in vitro* 4D Flow MRI and numerical simulation. *J Biomech*. 2015;48:1325–1330. doi: 10.1016/j.jbiomech.2015.03.009.

35. de Leval MR, Dubini G, Migliavacca F, Jalali H, Camporini G, Redington A, Pietrabissa R. Use of computational fluid dynamics in the design of surgical procedures: application to the study of competitive flows in cavopulmonary connections. *J Thorac Cardiovasc Surg*. 1996;111:502–513.

36. Healy TM, Lucas C, Yoganathan AP. Noninvasive fluid dynamic power loss assessments for total cavopulmonary connections using the viscous dissipation function: a feasibility study. *J Biomech Eng*. 2001;123:317–324.

37. Bolzon G, Pedrizzetti G, Grigioni M, Zovatto L, Daniele C, D'Avenio G. Flow on the symmetry plane of a total cavo-pulmonary connection. *J Biomech*. 2002;35:595–608.

38. DeGroff CG, Shandas R. Designing the optimal total cavopulmonary connection: pulsatile versus steady flow experiments. *Med Sci Monit*. 2002;8:MT41–MT45.

39. Bove EL, de Leval MR, Migliavacca F, Guadagni G, Dubini G. Computational fluid dynamics in the evaluation of hemodynamic performance of cavopulmonary connections after the Norwood procedure for hypoplastic left heart syndrome. *J Thorac Cardiovasc Surg*. 2003;126:1040–1047. doi: 10.1016/S0022.

40. Hsia TY, Migliavacca F, Pittaccio S, Radaelli A, Dubini G, Pennati G, de Leval M. Computational fluid dynamic study of flow optimization in realistic models of the total cavopulmonary connections. *J Surg Res*. 2004;116:305–313. doi: 10.1016/j.jss.2003.08.004.

41. Liu Y, Pekkan K, Jones SC, Yoganathan AP. The effects of different mesh generation methods on computational fluid dynamic analysis and power loss assessment in total cavopulmonary connection. *J Biomech Eng*. 2004;126:594–603.

42. Pekkan K, Kitajima HD, de Zelicourt D, Forbess JM, Parks WJ, Fogel MA, Sharma S, Kanter KR, Frakes D, Yoganathan AP. Total cavopulmonary connection flow with functional left pulmonary artery stenosis: angio-

43. plasty and fenestration *in vitro*. *Circulation*. 2005;112:3264–3271. doi: 10.1161/CIRCULATIONAHA.104.530931.

43. Moyle KR, Mallinson GD, Occleshaw CJ, Cowan BR, Gentles TL. Wall shear stress is the primary mechanism of energy loss in the Fontan connection. *Pediatr Cardiol*. 2006;27:309–315. doi: 10.1007/s00246-005-0918-3.

44. Orlando W, Shandas R, DeGroff C. Efficiency differences in computational simulations of the total cavo-pulmonary circulation with and without compliant vessel walls. *Comput Methods Programs Biomed*. 2006;81:220–227. doi: 10.1016/j.cmpb.2005.11.010.

45. Marsden AL, Vignon-Clementel IE, Chan FP, Feinstein JA, Taylor CA. Effects of exercise and respiration on hemodynamic efficiency in CFD simulations of the total cavopulmonary connection. *Ann Biomed Eng*. 2007;35:250–263. doi: 10.1007/s10439-006-9224-3.

46. Whitehead KK, Pekkan K, Kitajima HD, Paridon SM, Yoganathan AP, Fogel MA. Nonlinear power loss during exercise in single-ventricle patients after the Fontan: insights from computational fluid dynamics. *Circulation*. 2007;116(11 Suppl):I165–I171. doi: 10.1161/CIRCULATIONAHA.106.680827.

47. Sundareswaran KS, Pekkan K, Dasi LP, Whitehead K, Sharma S, Kanter KR, Fogel MA, Yoganathan AP. The total cavopulmonary connection resistance: a significant impact on single ventricle hemodynamics at rest and exercise. *Am J Physiol Heart Circ Physiol*. 2008;295:H2427–H2435. doi: 10.1152/ajpheart.00628.2008.

48. Itatani K, Miyaji K, Tomoyasu T, Nakahata Y, Ohara K, Takamoto S, Ishii M. Optimal conduit size of the extracardiac Fontan operation based on energy loss and flow stagnation. *Ann Thorac Surg*. 2009;88:565–572. doi: 10.1016/j.athoracsur.2009.04.109.

49. Marsden AL, Bernstein AJ, Reddy VM, Shadden SC, Spilker RL, Chan FP, Taylor CA, Feinstein JA. Evaluation of a novel Y-shaped extracardiac Fontan baffle using computational fluid dynamics. *J Thorac Cardiovasc Surg*. 2009;137:394.e2–403.e2. doi: 10.1016/j.jtcvs.2008.06.043.

50. Marsden AL, Reddy VM, Shadden SC, Chan FP, Taylor CA, Feinstein JA. A new multiparameter approach to computational simulation for Fontan assessment and redesign. *Congenit Heart Dis*. 2010;5:104–117. doi: 10.1111/j.1747-0803.2010.00383.x.

51. Baretta A, Corsini C, Yang W, Vignon-Clementel IE, Marsden AL, Feinstein JA, Hsia TY, Dubini G, Migliavacca F, Pennati G; Modeling of Congenital Hearts Alliance (MOCHA) Investigators. Virtual surgeries in patients with congenital heart disease: a multi-scale modelling test case. *Philos Trans A Math Phys Eng Sci*. 2011;369:4316–4330. doi: 10.1098/rsta.2011.0130.

52. Dasi LP, Whitehead K, Pekkan K, de Zelicourt D, Sundareswaran K, Kanter K, Fogel MA, Yoganathan AP. Pulmonary hepatic flow distribution in total cavopulmonary connections: extracardiac versus intracardiac. *J Thorac Cardiovasc Surg*. 2011;141:207–214. doi: 10.1016/j.jtcvs.2010.06.009.

53. Itatani K, Miyaji K, Nakahata Y, Ohara K, Takamoto S, Ishii M. The lower limit of the pulmonary artery index for the extracardiac Fontan circulation. *J Thorac Cardiovasc Surg*. 2011;142:127–135. doi: 10.1016/j.jtcvs.2010.11.033.

54. Haggerty CM, de Zélicourt DA, Restrepo M, Rossignac J, Spray TL, Kanter KR, Fogel MA, Yoganathan AP. Comparing pre- and post-operative Fontan hemodynamic simulations: implications for the reliability of surgical planning. *Ann Biomed Eng*. 2012;40:2639–2651. doi: 10.1007/s10439-012-0614-4.

55. Khiabani RH, Restrepo M, Tang E, De Zélicourt D, Sotiropoulos F, Fogel M, Yoganathan AP. Effect of flow pulsatility on modeling the hemodynamics in the total cavopulmonary connection. *J Biomech*. 2012;45:2376–2381. doi: 10.1016/j.jbiomech.2012.07.010.

56. Ding J, Liu Y, Wang F. Influence of bypass angles on extracardiac Fontan connections: a numerical study. *Int J Numer Method Biomed Eng*. 2013;29:351–362. doi: 10.1002/cnm.2508.

57. Haggerty CM, Kanter KR, Restrepo M, de Zélicourt DA, Parks WJ, Rossignac J, Fogel MA, Yoganathan AP. Simulating hemodynamics of the Fontan Y-graft based on patient-specific *in vivo* connections. *J Thorac Cardiovasc Surg*. 2013;145:663–670. doi: 10.1016/j.jtcvs.2012.03.076.

58. Kung E, Baretta A, Baker C, Arbia G, Biglino G, Corsini C, Schievano S, Vignon-Clementel IE, Dubini G, Pennati G, Taylor A, Dorfman A, Hlavacek AM, Marsden AL, Hsia TY, Migliavacca F; Modeling Of Congenital Hearts Alliance I. Predictive modeling of the virtual Hemi-Fontan operation for second stage single ventricle palliation: two patient-specific cases. *J Biomech*. 2013;46:423–429.

59. Bossers SS, Cibis M, Gijsen FJ, Schokking M, Strengers JL, Verhaart RF, Moelker A, Wentzel JJ, Helbing WA. Computational fluid dynamics in Fontan patients to evaluate power loss during simulated exercise. *Heart*. 2014;100:696–701. doi: 10.1136/heartjnl-2013-304969.

60. Haggerty CM, Restrepo M, Tang E, de Zélicourt DA, Sundareswaran KS, Mirabella L, Bethel J, Whitehead KK, Fogel MA, Yoganathan AP. Fontan hemodynamics from 100 patient-specific cardiac magnetic resonance studies: a computational fluid dynamics analysis. *J Thorac Cardiovasc Surg*. 2014;148:1481–1489. doi: 10.1016/j.jtcvs.2013.11.060.

61. Tang E, Restrepo M, Haggerty CM, Mirabella L, Bethel J, Whitehead KK, Fogel MA, Yoganathan AP. Geometric characterization of patient-specific total cavopulmonary connections and its relationship to hemodynamics. *JACC Cardiovasc Imaging*. 2014;7:215–224. doi: 10.1016/j.jcmg.2013.12.010.

62. Haggerty CM, Whitehead KK, Bethel J, Fogel MA, Yoganathan AP. Relationship of single ventricle filling and preload to total cavopulmonary connection hemodynamics. *Ann Thorac Surg*. 2015;99:911–917. doi: 10.1016/j.athoracsur.2014.10.043.

63. Khiabani RH, Whitehead KK, Han D, Restrepo M, Tang E, Bethel J, Paridon SM, Fogel MA, Yoganathan AP. Exercise capacity in single-ventricle patients after Fontan correlates with haemodynamic energy loss in TCPC. *Heart*. 2015;101:139–143. doi: 10.1136/heartjnl-2014-306337.

64. Restrepo M, Tang E, Haggerty CM, Khiabani RH, Mirabella L, Bethel J, Valente AM, Whitehead KK, McElhinney DB, Fogel MA, Yoganathan AP. Energetic implications of vessel growth and flow changes over time in Fontan patients. *Ann Thorac Surg*. 2015;99:163–170. doi: 10.1016/j.athoracsur.2014.08.046.

65. Trusty PM, Restrepo M, Kanter KR, Yoganathan AP, Fogel MA, Slesnick TC. A pulsatile hemodynamic evaluation of the commercially available bifurcated Y-graft Fontan modification and comparison with the lateral tunnel and extracardiac conduits. *J Thorac Cardiovasc Surg*. 2016;151:1529–1536. doi: 10.1016/j.jtcvs.2016.03.019.

66. Tang E, Wei ZA, Whitehead KK, Khiabani RH, Restrepo M, Mirabella L, Bethel J, Paridon SM, Marino BS, Fogel MA, Yoganathan AP. Effect of Fontan geometry on exercise haemodynamics and its potential implications. *Heart*. 2017;103:1806–1812. doi: 10.1136/heartjnl-2016-310855.

67. Wei ZA, Trusty PM, Tree M, Haggerty CM, Tang E, Fogel M, Yoganathan AP. Can time-averaged flow boundary conditions be used to meet the clinical timeline for Fontan surgical planning? *J Biomech*. 2017;50:172–179. doi: 10.1016/j.jbiomech.2016.11.025.

68. Sharma S, Ensley AE, Hopkins K, Chatzimavroudis GP, Healy TM, Tam VK, Kanter KR, Yoganathan AP. In vivo flow dynamics of the total cavopulmonary connection from three-dimensional multislice magnetic resonance imaging. *Ann Thorac Surg*. 2001;71:889–898.

69. Honda T, Itatani K, Takanashi M, Mineo E, Kitagawa A, Ando H, Kimura S, Nakahata Y, Oka N, Miyaji K, Ishii M. Quantitative evaluation of hemodynamics in the Fontan circulation: a cross-sectional study measuring energy loss in vivo. *Pediatr Cardiol*. 2014;35:361–367. doi: 10.1007/s00246-013-0783-4.

70. Cibis M, Jarvis K, Markl M, Rose M, Rigsby C, Barker AJ, Wentzel JJ. The effect of resolution on viscous dissipation measured with 4D flow MRI in patients with Fontan circulation: Evaluation using computational fluid dynamics. *J Biomech*. 2015;48:2984–2989. doi: 10.1016/j.jbiomech.2015.07.039.

71. Ascuitto RJ, Kydon DW, Ross-Ascuitto NT. Pressure loss from flow energy dissipation: relevance to Fontan-type modifications. *Pediatr Cardiol*. 2001;22:110–115. doi: 10.1007/s002460010172.

72. Sundareswaran KS, Haggerty CM, de Zélicourt D, Dasi LP, Pekkan K, Frakes DH, Powell AJ, Kanter KR, Fogel MA, Yoganathan AP. Visualization of flow structures in Fontan patients using 3-dimensional phase contrast magnetic resonance imaging. *J Thorac Cardiovasc Surg*. 2012;143:1108–1116. doi: 10.1016/j.jtcvs.2011.09.067.

73. Migliavacca F, Dubini G, Bove EL, de Leval MR. Computational fluid dynamics simulations in realistic 3-D geometries of the total cavopulmonary anastomosis: the influence of the inferior caval anastomosis. *J Biomech Eng*. 2003;125:805–813.

74. Yang W, Vignon-Clementel IE, Troianowski G, Reddy VM, Feinstein JA, Marsden AL. Hepatic blood flow distribution and performance in conventional and novel Y-graft Fontan geometries: a case series computational fluid dynamics study. *J Thorac Cardiovasc Surg*. 2012;143:1086–1097. doi: 10.1016/j.jtcvs.2011.06.042.

75. Hong H, Menon PG, Zhang H, Ye L, Zhu Z, Chen H, Liu J. Postsurgical comparison of pulsatile hemodynamics in five unique total cavopulmonary connections: identifying ideal connection strategies. *Ann Thorac Surg*. 2013;96:1398–1404. doi: 10.1016/j.athoracsur.2013.05.035.

76. Sun Q, Liu J, Qian Y, Zhang H, Wang Q, Sun Y, Hong H, Liu J. Computational haemodynamic analysis of patient-specific virtual operations for total cavopulmonary connection with dual superior venae cavae. *Eur J Cardiothorac Surg*. 2014;45:564–569. doi: 10.1093/ejcts/ezt394.

77. Goldstein BH, Connor CE, Gooding L, Rocchini AP. Relation of systemic venous return, pulmonary vascular resistance, and diastolic dysfunction to exercise capacity in patients with single ventricle receiving fontan palliation. *Am J Cardiol*. 2010;105:1169–1175. doi: 10.1016/j.amjcard.2009.12.020.

78. DeGroff CG, Carlton JD, Weinberg CE, Ellison MC, Shandas R, Valdes-Cruz L. Effect of vessel size on the flow efficiency of the total cavopulmonary connection: in vitro studies. *Pediatr Cardiol*. 2002;23:171–177. doi: 10.1007/s00246-001-0042-y.

79. Dasi LP, Krishnankuttyrema R, Kitajima HD, Pekkan K, Sundareswaran KS, Fogel M, Sharma S, Whitehead K, Kanter K, Yoganathan AP. Fontan hemodynamics: importance of pulmonary artery diameter. *J Thorac Cardiovasc Surg*. 2009;137:560–564. doi: 10.1016/j.jtcvs.2008.04.036.

80. de Zélicourt DA, Kurtcuoglu V. Patient-specific surgical planning, where do we stand? The example of the Fontan procedure. *Ann Biomed Eng*. 2016;44:174–186. doi: 10.1007/s10439-015-1381-9.

81. van Brakel TJ, Schoof PH, de Roo F, Nikkels PG, Evens FC, Haas F. High incidence of Dacron conduit stenosis for extracardiac Fontan procedure. *J Thorac Cardiovasc Surg*. 2014;147:1568–1572. doi: 10.1016/j.jtcvs.2013.07.013.

82. Tang E, McElhinney DB, Restrepo M, Valente AM, Yoganathan AP. Haemodynamic impact of stent implantation for lateral tunnel Fontan stenosis: a patient-specific computational assessment. *Cardiol Young*. 2016;26:116–126. doi: 10.1017/S1047951114002765.

83. Salim MA, DiSessa TG, Arheart KL, Alpert BS. Contribution of superior vena caval flow to total cardiac output in children: a Doppler echocardiographic study. *Circulation*. 1995;92:1860–1865.

84. Wei Z, Whitehead KK, Khiabani RH, Tree M, Tang E, Paridon SM, Fogel MA, Yoganathan AP. Respiratory effects on Fontan circulation during rest and exercise using real-time cardiac magnetic resonance imaging. *Ann Thorac Surg*. 2016;101:1818–1825. doi: 10.1016/j.athoracsur.2015.11.011.

85. Pedersen EM, Stenbøg EV, Fründ T, Houlind K, Kromann O, Sørensen KE, Emmertsen K, Hjortdal VE. Flow during exercise in the total cavopulmonary connection measured by magnetic resonance velocity mapping. *Heart*. 2002;87:554–558.

86. Soerensen DD, Pekkan K, Sundareswaran KS, Yoganathan AP. New power loss optimized Fontan connection evaluated by calculation of power loss using high resolution PC-MRI and CFD. *Conf Proc IEEE Eng Med Biol Soc*. 2004;2:1144–1147. doi: 10.1109/IEMBS.2004.1403367.

87. Trusty PM, Wei Z, Tree M, Kanter KR, Fogel MA, Yoganathan AP, Slesnick TC. Local hemodynamic differences between commercially available Y-grafts and traditional Fontan baffles under simulated exercise conditions: implications for exercise tolerance. *Cardiovasc Eng Technol*. 2017;8:390–399. doi: 10.1007/s13239-017-0310-5.

88. Desai K, Haggerty CM, Kanter KR, Rossignac J, Spray TL, Fogel MA, Yoganathan AP. Haemodynamic comparison of a novel flow-divider Optiflo geometry and a traditional total cavopulmonary connection. *Interact Cardiovasc Thorac Surg*. 2013;17:1–7. doi: 10.1093/icvts/ivt099.

89. Arbia G, Corsini C, Esmaily Moghadam M, Marsden AL, Migliavacca F, Pennati G, Hsia TY, Vignon-Clementel IE; Modeling Of Congenital Hearts Alliance (MOCHA) Investigators. Numerical blood flow simulation in surgical corrections: what do we need for an accurate analysis? *J Surg Res*. 2014;186:44–55. doi: 10.1016/j.jss.2013.07.037.

90. Masters JC, Ketner M, Bleiweis MS, Mill M, Yoganathan A, Lucas CL. The effect of incorporating vessel compliance in a computational model of blood flow in a total cavopulmonary connection (TCPC) with caval centerline offset. *J Biomech Eng*. 2004;126:709–713.

91. Biglino G, Capelli C, Bruse J, Bosi GM, Taylor AM, Schievano S. Computational modelling for congenital heart disease: how far are we from clinical translation? *Heart*. 2017;103:98–103. doi: 10.1136/heartjnl-2016-310423.

92. Tree M, Wei ZA, Trusty PM, Raghav V, Fogel M, Maher K, Yoganathan A. Using a novel in vitro Fontan model and condition-specific real-time MRI data to examine hemodynamic effects of respiration and exercise. *Ann Biomed Eng*. 2018;46:135–147. doi: 10.1007/s10439-017-1943-0.

93. Roldán-Alzate A, García-Rodríguez S, Anagnostopoulos PV, Srinivasan S and Francois CJ. Kinetic energy efficiency of single ventricle and TCPC using 4D flow MRI. *Journal of Cardiovascular Magnetic Resonance*. 2015;17.

94. Wei ZA, Tree M, Trusty PM, Wu W, Singh-Gryzbon S, Yoganathan A. The advantages of viscous dissipation rate over simplified power loss as a Fontan hemodynamic metric. *Ann Biomed Eng*. 2018;46:404–416. doi: 10.1007/s10439-017-1950-1.

95. Sjöberg P, Heiberg E, Wingren P, Ramgren Johansson J, Malm T, Arheden H, Liuba P, Carlsson M. Decreased diastolic ventricular kinetic energy in

young patients with Fontan circulation demonstrated by four-dimensional cardiac magnetic resonance imaging. *Pediatr Cardiol*. 2017;38:669–680. doi: 10.1007/s00246-016-1565-6.

96. Giardini A, Hager A, Pace Napoleone C, Picchio FM. Natural history of exercise capacity after the Fontan operation: a longitudinal study. *Ann Thorac Surg*. 2008;85:818–821. doi: 10.1016/j.athoracsur.2007.11.009.

97. Gewillig M, Brown SC. The Fontan circulation after 45 years: update in physiology. *Heart*. 2016;102:1081–1086. doi: 10.1136/heartjnl-2015-307467.

98. Naeije R, Chesler N. Pulmonary circulation at exercise. *Compr Physiol*. 2012;2:711–741. doi: 10.1002/cphy.c100091.

99. Khiabani RH, Whitehead KK, Han D, Restrepo M, Tang E, Bethel J, Paridon SM, Fogel MA, Yoganathan AP. Does TCPC power loss really affect exercise capacity? *Heart*. 2015;101:575–576. doi: 10.1136/heartjnl-2015-307484.

100. Cavalcanti S, Gnudi G, Masetti P, Ussia GP, Marcelletti CF. Analysis by mathematical model of haemodynamic data in the failing Fontan circulation. *Physiol Meas*. 2001;22:209–222.